

## Time-resolved small-angle neutron scattering during heat-induced fibril formation from bovine $\beta$ -lactoglobulin

Luben N. Arnaudov<sup>a)</sup> and Renko de Vries

Laboratory of Physical Chemistry and Colloid Science, Wageningen University, Dreijenplein 6, 6700 EK Wageningen, The Netherlands and Food Physics Group, Wageningen University, Bomenweg 2, 6703 HD Wageningen, The Netherlands

Martien A. Cohen Stuart

Laboratory of Physical Chemistry and Colloid Science, Wageningen University, Dreijenplein 6, 6700 EK Wageningen, The Netherlands

(Received 29 November 2005; accepted 6 January 2006; published online 22 February 2006)

We study *in situ* the kinetics of heat-induced fibrillar aggregation of bovine  $\beta$ -lactoglobulin at  $pH$  2.0 and 80 °C for the first time by time-resolved small-angle neutron scattering. A simple model for the scattering from a mixture of monodisperse charged spheres (monomeric  $\beta$ -lactoglobulin) interacting via a screened electrostatic repulsion and noninteracting long cylinders (protein fibrils) is used to describe the data. The experimental data are fitted to the model and the concentration of the monomeric protein and the protein incorporated in fibrils are obtained as adjustable parameters. Thus, a simple physical model allows the determination of realistic kinetic parameters during fibrillar protein aggregation. This result constitutes an important step in understanding the process of irreversible fibrillar aggregation of proteins. © 2006 American Institute of Physics.

[DOI: [10.1063/1.2171418](https://doi.org/10.1063/1.2171418)]

### INTRODUCTION

In a previous study<sup>1</sup> we have shown that the process of heat-induced fibril formation from bovine  $\beta$ -lactoglobulin ( $\beta$ -lg) at  $pH$  2.0 is a multistep process which is partially reversible upon slow cooling. We have also shown that two simultaneous reactions proceed during heating: the first one leads to the fibril formation and the other one is the complete denaturation of the protein molecules that renders them incapable of further aggregation.<sup>1–3</sup> The competition between these two processes manifests itself as an apparent critical aggregation concentration that depends on the ionic strength of the solution.<sup>1–3</sup>

To better understand the kinetics of fibrillar aggregation of  $\beta$ -lg the most important information that is needed is the time dependence of the concentration of the monomeric protein and the concentration of the protein included in the fibrils. The present study aims at obtaining such quantitative information by using time-resolved small-angle neutron scattering (SANS) from heated  $\beta$ -lg solutions at low ionic strength and  $pH$  2.0.

So far the studies of the fibrillar aggregation of  $\beta$ -lg by SANS have been carried out *ex situ*, i.e., on quenched samples at ambient temperature.<sup>4,5</sup> Such an approach can only give information about the state of the studied solution under the conditions where data are taken, i.e., monomer protein concentration and concentration of aggregates, after a cooling step and possibly after a dilution step. To obtain information about the true kinetics of the process one needs

to study it *in situ* without disturbing the main parameters of the process, i.e., protein concentration,  $pH$ , temperature, and ionic strength. A number of *in situ* studies of the fibrillar aggregation of  $\beta$ -lg have been carried out by using light scattering (LS).<sup>2,3,6–8</sup> LS is an extremely sensitive and precise technique but has some disadvantages. The main disadvantage for studying fibrillar aggregation by LS is that in the  $q$  range in which a typical LS setup is operative the long rodlike aggregates quickly dominate the scattering and the quantitative interpretation of the experiment is greatly complicated. On the other hand, experimental methods such as small-angle x-ray and neutron scatterings allow covering a wider  $q$  range, and also allow discriminating between the contributions from particles of different shapes and sizes to the scattering. Since there is no radiation damage to the sample when cold neutrons are used one can probe the long-time kinetics by SANS. One can also obtain the maximum scattering contrast by dissolving the protein in heavy water.

In the present study we investigate the kinetics of fibrillar aggregation of  $\beta$ -lg at  $pD$  2.0 and  $T=80$  °C by time-resolved SANS. We obtain the absolute differential cross section for the neutrons scattered from the samples and the data are processed with the help of a simple model for scattering from interacting charged spherical macroions (protein molecules) and noninteracting cylindrical aggregates (fibrils). Good agreement between the model and the experimental data is obtained. The concentrations of the free monomers and the protein molecules incorporated into fibrils are obtained as adjustable parameters by nonlinear least-squares fitting.

<sup>a)</sup> Author to whom correspondence should be addressed. Electronic mail: [luben.arnaudov@wur.nl](mailto:luben.arnaudov@wur.nl)

## MATERIALS AND METHODS

### Sample preparation

Bovine  $\beta$ -lactoglobulin was obtained from Sigma ( $3\times$  crystallized and lyophilized, Ref. L0130, Lot 21K7079). It is a mixture of genetic variants *A* and *B*, and is used throughout all experiments. The protein was extensively dialyzed against de-ionized water (Barnstead) in the presence of 200 ppm  $\text{NaN}_3$  to prevent bacterial growth, and subsequently freeze-dried. All solutions were prepared by dissolving the freeze-dried protein in  $\text{D}_2\text{O}$  (Sigma) and contained 200 ppm  $\text{NaN}_3$ . The *pD* was adjusted by addition of small quantities of 1M DCl solution prepared by dissolving 35% DCl (Sigma) in  $\text{D}_2\text{O}$ . The *pD* was measured by a normal *pH* electrode and was corrected according to the expression  $pD = pH + 0.4$ . Three concentrations were prepared and filtered through 0.1  $\mu\text{m}$  low protein adsorbing filters into clean glass tubes. The protein concentration in the filtered samples was determined by UV spectrophotometry at 278 nm using an extinction coefficient of 0.83  $\text{L g}^{-1} \text{cm}^{-1}$ . For the neutron scattering 1 ml of each concentration was transferred into clean 2 mm path length quartz cells (404.000-QX, Hellma, Germany).

### SANS measurements

SANS was performed on the SANS I instrument at the SINQ facility of the Paul Scherrer Institute, Villigen, Switzerland. Two sample-to-detector distances were used, 2 and 11 m, with respective collimations of 6 and 11 m. The wavelength of the neutrons used throughout all measurements was 6  $\text{\AA}$  with  $\Delta\lambda/\lambda = 10\%$  full width at half maximum (FWHM). The  $q$  range covered was  $5.3 \times 10^{-3} - 0.34 \text{ \AA}^{-1}$ . The scattering cells were mounted in a thermostated cell holder at 25  $^\circ\text{C}$  during the test and calibration measurements. Subsequently, the temperature was raised to 80  $^\circ\text{C}$  and the scattering of the solvent at both instrument configurations was measured. After that, the samples with the protein solutions were quickly introduced in the preheated sample holder, one at a time, and the scattering was recorded for a period of 5 h. Experiments with identical protein concentrations were carried out twice, at 2 and 11 m sample-to-detector distances. The temperature was measured inside an identical quartz cell positioned next to the sample cell. In the case of the 2 m sample-to-detector distance, spectra were collected (in separate files) every 5 min. In the case of the 11 m sample-to-detector distance, spectra were collected every 15 min to ensure a good signal-to-noise ratio. After each experimental run the aggregation was quenched by introducing the sample cell into ice-cold water and the sample was subsequently transferred into a clean cell for further evaluation.

The data reduction was carried out using the GRASP V. 3.991 software developed at the Institute Laue-Langevin (ILL) in Grenoble, France. The data were corrected for background and empty cell scatterings. Absolute calibration was performed by using the incoherent scattering of  $\text{H}_2\text{O}$  at 2 m sample-to-detector distance with 6 m collimation. For the 11 m sample-to-detector distance corrections for the neutron flux and the solid angle were made.

## THEORETICAL BACKGROUND

In SANS one measures the differential scattering cross section per unit volume, which in the case of scattering from a solution containing  $p$  different species can be written as<sup>9,10</sup>

$$\frac{d\Sigma(q)}{d\Omega} = \Delta\rho^2 \left\{ \sum_{i=1}^p n_i V_i^2 [\langle F_i^2(q) \rangle - \langle F_i(q) \rangle^2] + \sum_{i,j=1}^p \sqrt{n_i n_j} V_i V_j \langle F_i(q) \rangle \langle F_j(q) \rangle S_{ij}(q) \right\}, \quad (1)$$

where  $q$  is the scattering wave vector with magnitude  $q = (4\pi/\lambda)\sin\theta$ ;  $\lambda$  is the incident-beam wavelength;  $2\theta$  is the scattering angle;  $\Delta\rho = \rho_p - \rho_0$  is the scattering contrast, with  $\rho_p$  the scattering length density of the scattering species (protein molecules) and  $\rho_0$  the scattering length density of the solvent;  $n_i$  is the number concentration of the  $i$  species;  $V_i$  is the volume of the  $i$  species;  $F_i(q)$  are the form factors of the  $i$  species; and  $S_{ij}(q)$  are the partial structure factors due to the interaction between species  $i$  and  $j$ . The angular brackets denote orientation averaging. In our case of fibrillar aggregation we consider the system consisting only of two species—monomeric protein  $m$  and fibrillar protein  $f$ . In that case Eq. (1) reads

$$\begin{aligned} \frac{d\Sigma(q,t)}{d\Omega} = & \Delta\rho^2 \{ n_m(t) V_m^2 P_m(q) S_{mm}(q, n_m(t)) \} \\ & + \Delta\rho^2 \{ \sqrt{n_m(t) n_f(t)} V_m V_f(t) \langle F_m(q) \rangle \langle F_f(q,t) \rangle \\ & + n_f(t) V_f^2(t) P_f(q,t) \}, \end{aligned} \quad (2)$$

where  $n_m(t)$  and  $n_f(t)$  are the number concentrations of the monomeric protein and fibrils, and  $V_m$  and  $V_f(t)$  are the respective volumes occupied by one monomer and one fibril.  $\langle F_m(q) \rangle$  is the orientation-averaged form factor due to monodisperse spherical monomeric protein with a radius  $R$ :<sup>11</sup>

$$\langle F_m(q) \rangle = \frac{3(\sin(qR) - qR \cos(qR))}{q^3 R^3}. \quad (3)$$

Actually, for homogeneous spheres, the orientation average does not change the form factor, because of the spherical symmetry of the scattering objects.  $\langle F_f(q) \rangle$  is the orientation-averaged form factor due to cylinders with radii equal to the radius of the monomeric protein,  $R$ , and time-dependent average length  $L = 2R \langle N(t) \rangle$ ,  $\langle N(t) \rangle$  being the mean aggregation number of the fibrils:

$$\langle F_m(q) \rangle = \int_0^{\pi/2} \frac{2J_1(qR \sin \alpha) \sin[(qL \cos \alpha)/2]}{qR \sin \alpha (qL \cos \alpha)/2} \sin \alpha d\alpha, \quad (4)$$

where  $J_1(x)$  is the Bessel function of first order.<sup>10</sup>  $P_m(q) = \langle F_m^2(q) \rangle \equiv \langle F_m(q) \rangle^2$  is the orientation-averaged amplitude of the form factor due to monodisperse homogeneous spheres with radius  $R$ . Finally,  $P_f(q)$  is the averaged amplitude of the form factor due to cylindrical aggregates:

$$P_f(q) = \int_0^{\pi/2} \left[ \frac{2J_1(qR \sin \alpha) \sin[(qL \cos \alpha)/2]}{qR \sin \alpha (qL \cos \alpha)/2} \right]^2 \sin \alpha d\alpha. \quad (5)$$

We assume that the only structure factor different from unity is the structure factor due to the protein-protein interaction. At the beginning of the aggregation process there are only protein monomers in the solution and in the early stages of the aggregation process the concentration of the fibrils is very low. That is why our assumption for the structure factors is justified, especially for the early stages of the aggregation process. The protein monomers at pH 2.0 are considered as spherical particles with about 20 uniformly distributed positive charges. We consider the interaction potential between them to be that of hard-core spheres with a screened electrostatic tail, which can be written as

$$U(r) = \frac{Z^2 e^2}{4\pi\epsilon_0(1 + \kappa R)^2} \frac{\exp(-\kappa(r - 2R))}{r}, \quad r > 2R \quad (6)$$

$$U(r) = \infty, \quad r < 2R,$$

where  $Z$  is the number of charges per molecule,  $e$  is the elementary electron charge,  $\epsilon_0$  is the dielectric permittivity of vacuum,  $\epsilon$  is the relative dielectric permittivity of the medium,  $\kappa$  is the inverse Debye screening length, and  $R$  is the radius of the particles. An analytical expression for the structure factor of macroion solutions interacting with a screened electrostatic repulsion potential of the form (6) is obtained by Hayter and Penfold<sup>12</sup> as a solution of the Ornstein-Zernike equation in mean spherical approximation. Since we work at relatively low protein concentrations we calculate the structure factor using the procedure known as the rescaled mean spherical approximation, described by Hansen and Hayter.<sup>13</sup>

## FITTING PROCEDURE

The experimental data were fitted to the model described above so that information about the kinetics of the fibrillar aggregation of  $\beta$ -Ig at pH 2.0 could be extracted. The fitting was carried out on the spectra collected at consecutive times using a nonlinear least-squares method on the merit function:<sup>14</sup>

$$\chi^2 = \sum_{i=1}^k \left[ \frac{(d\Sigma(q_i)/d\Omega)_{\text{exp}} - (d\Sigma(q_i)/d\Omega)_{\text{mod}}^{\text{sm}} - B_{\text{inc}}}{\sigma_i} \right]^2, \quad (7)$$

where  $k$  is the number of experimental points in the spectrum, the parameter  $B_{\text{inc}}$  accounts for a flat incoherent background, and  $\sigma_i$  are the standard deviations of the experimental data. The model cross section was calculated by using Eq. (2) and was smeared with the instrument resolution  $R(q, q_i)$  by the following expression:<sup>10</sup>

$$(d\Sigma(q_i)/d\Omega)_{\text{mod}}^{\text{sm}} = \int (d\Sigma(q)/d\Omega)_{\text{mod}} R(q, q_i) dq. \quad (8)$$

The main adjustable parameters were the monomer protein concentration  $n_m(t_j)$  and the mean aggregation number of the fibrils  $\langle N(t_j) \rangle$  for each collected spectrum  $j$ . A small adjust-

ment was made to the scattering contrast for each concentration series by using the data from the first file of the series because of the impossibility to precisely calculate the effect of the hydrogen-deuterium exchange in the protein molecules on the scattering length density of the protein. The concentration of protein fibrils was calculated by the following expression:

$$n_f(t_j) = \frac{n_0 - n_m(t_j)}{\langle N(t_j) \rangle}, \quad (9)$$

where  $n_0$  is the number concentration of protein monomers before the heating had started. The diameter of the fibrils was assumed to be equal to the diameter of the monomeric protein, which is acceptable considering the results for the fibril morphology from our previous studies.<sup>1</sup> For the fitting, a custom-made software was written in PASCAL by using adaptive Simpson quadrature<sup>14</sup> for calculating the cylinder form factors and the Nelder-Mead simplex algorithm for the optimization procedure.<sup>15</sup> The structure factor for the monomers was calculated by using the procedures described in Refs. 12 and 13.

## RESULTS AND DISCUSSION

Figure 1(a) shows all the curves for the differential scattering cross section of 6.75 wt %  $\beta$ -Ig solution, recorded during a period of 5 h at 80 °C. The first curve is recorded 11 min after the heating had started. One can see a well-distinguished peak due to the structure factor contribution from the monomeric protein. As the heating time increases one can see that the signal in the low- $q$  region goes up and after 5 h the peak disappears. This is due to the increasing amount of fibrils in the solution, and simultaneously decreasing amount of monomeric protein. The form factor of the long fibrils eventually dominates the low- $q$  region. The peak position due to the structure factor of monomeric protein should go to lower  $q$  values with decreasing concentration, and the peak magnitude should simultaneously decrease (as one can see in Fig. 5). In Fig. 1(b) part of the curves for the differential cross section obtained as best fits of the curves from Fig. 1(a) are plotted. One can see that the qualitative behavior of the curves is exactly the same as the one observed in Fig. 1(a). There is a slight difference in the shape of the curves in the low- $q$  region, as the curves from the numerical procedure show strictly  $q^{-1}$  behavior and those from the experiment are slightly bent upward. This may be due to two main factors. The first one is that our simple model considers monodisperse rods with some average length, while in reality the fibrils have a broad length distribution.<sup>16</sup> Including a form factor for polydisperse rods would undoubtedly improve the fit, but it would also increase the number of adjustable parameters. This affects the robustness of fit parameters and is, therefore, a bad practice; unless we have some independent means to determine the size distribution of the fibrils at any time, which we have not. The other factor that could affect the scattering at low  $q$  is the interaction between the charged aggregates or between aggregates and monomers. Including these interactions in the model would greatly complicate it. If no additional informa-



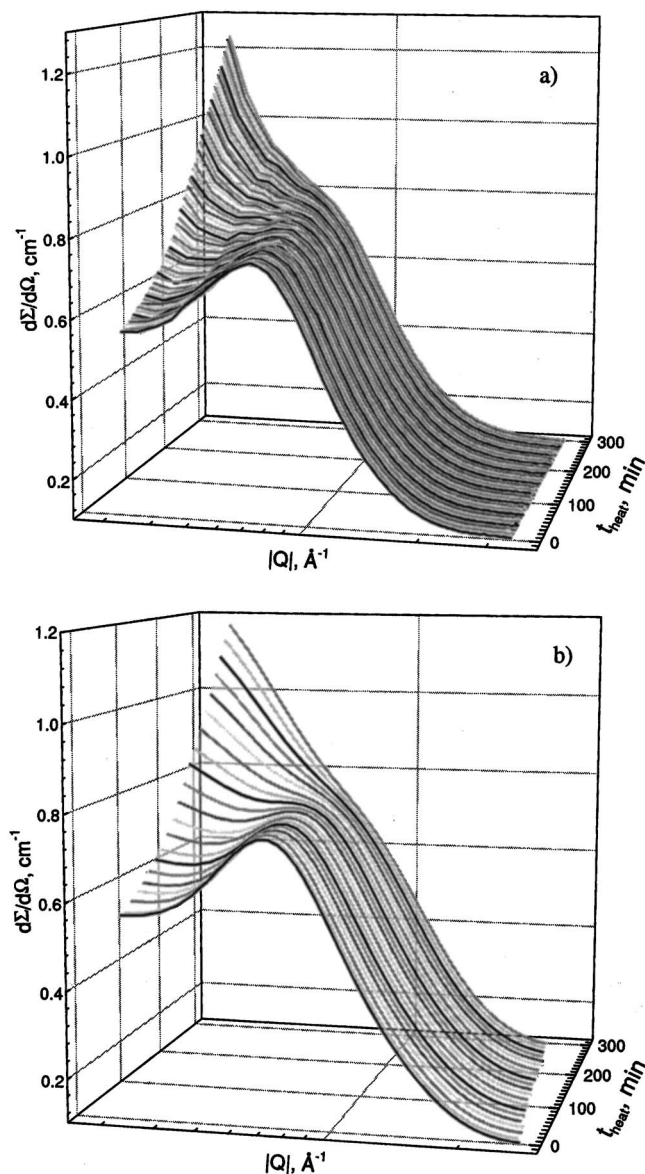


FIG. 1. (a) Experimental curves for the differential cross section for neutron scattering of 6.75 wt %  $\beta$ -Ig solution; (b) curves obtained as best fits of the experimental data in (a).

tion about the size and shape of the fibrils in solution are available, the above considerations about the robustness of the fit procedure hold.

An example of experimental data for 6.75 wt %  $\beta$ -Ig solution with the best-fit curves through them is plotted in Fig. 2. For clarity only six data sets are shown. One can see that the agreement between the experimental data and the theoretical model is excellent. Similar examples with data obtained from experiments with 4.14 and 2.33 wt %  $\beta$ -Ig solutions are shown in Figs. 3 and 4, respectively. One can see that with decreasing protein concentration the change in the scattering pattern becomes smaller. This is in agreement with our previous observations by proton NMR and light scattering and is caused by the apparent critical concentration for fibril formation.<sup>1-3</sup> In the case of 2.33 wt %  $\beta$ -Ig solution the change in the scattering data is only a little bigger than the experimental uncertainty. This is also in agreement with our previous results that show an apparent critical concentration of about 2 wt %.

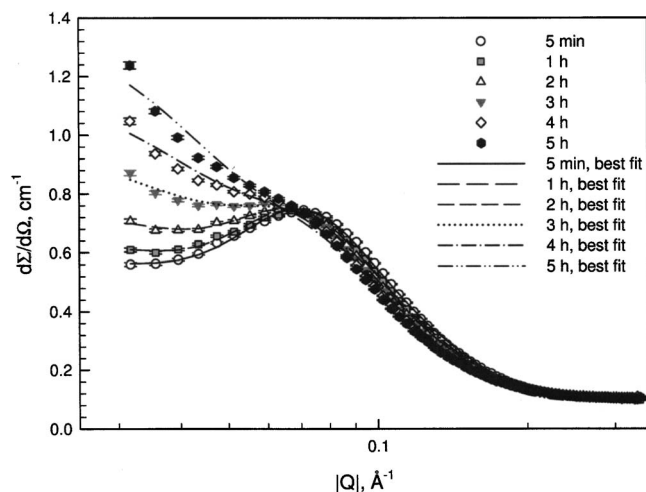


FIG. 2. Experimental data from SANS of 6.75 wt %  $\beta$ -Ig solution at six heating times indicated in the legend and best fits through the data.

Figure 5 shows the structure factors obtained from the fitting procedure for the three  $\beta$ -Ig concentrations just after the heating had started. The behavior mentioned earlier is clearly seen. The primary peak shifts towards lower  $q$ , consistently with the decreasing concentration of the interacting particles, and also the magnitude of the primary peak goes down. Thus our experimental data have enough degrees of freedom to obtain two adjustable parameters—the free monomer concentration and the concentration of monomers incorporated in the fibrils. Without additional information about the length distribution of the fibrils, obtaining the actual fibril concentration seems dubious.

Figure 6 shows the concentration of free monomers in the heated  $\beta$ -Ig solutions obtained as an adjustable parameter by the nonlinear least-squares fits for the three studied concentrations. The time dependence of the monomeric concentration is in semiquantitative agreement with our previous results by proton NMR spectroscopy and light scattering.<sup>1,2</sup> The most significant change in the monomer concentration is observed for the highest protein concentration. For the lowest protein concentration the change in the free monomer

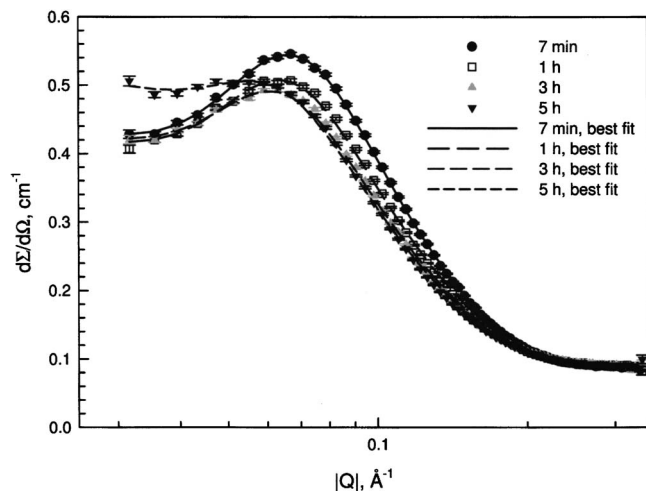


FIG. 3. Experimental data from SANS of 4.14 wt %  $\beta$ -Ig solution at four heating times indicated in the legend and best fits through the data.

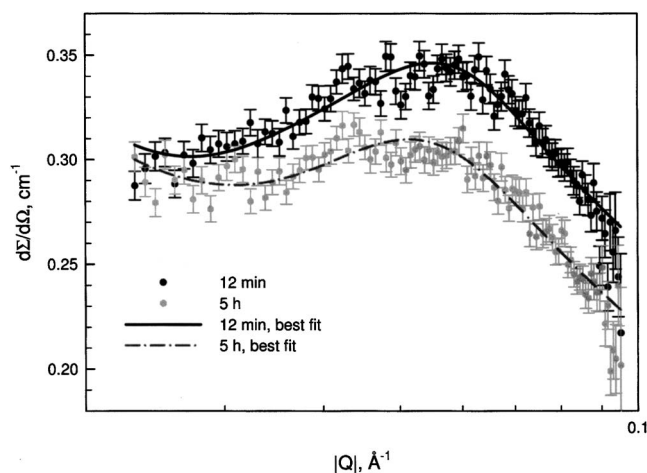


FIG. 4. Experimental data from SANS of 2.33 wt %  $\beta$ -lg solution at two heating times indicated in the legend and best fits through the data.

concentration is almost negligible within 5 h of heating. This is also consistent with the notion of an apparent critical concentration for fibril formation at about 2 wt %.<sup>1,2</sup>

One should be aware that when comparing data from different experimental techniques additional information should be taken into account. For example, in the case of NMR the solvent is water with 10% D<sub>2</sub>O, whereas in the case of SANS we use only D<sub>2</sub>O as a solvent. The obtained information are also method dependent. In the case of NMR the monomeric protein concentration is proportional to the intensity of the proton spectrum, and in the case of SANS the scattering data must be fitted by an appropriate model in order to obtain relevant information.

Finally, Fig. 7 shows the concentration of protein incorporated in the fibrils. These data are obtained from the data shown in Fig. 6 by using the constraint (9). This is valuable kinetic information, because it allows for modeling the kinetics of the protein aggregation for much longer times than the data obtained from light scattering.<sup>2</sup> In a previous study<sup>3</sup> we proposed a kinetic model for the fibril formation from  $\beta$ -lg at acidic pH and different ionic strengths that was valid for the early stages of the aggregation. As discussed there, to be able

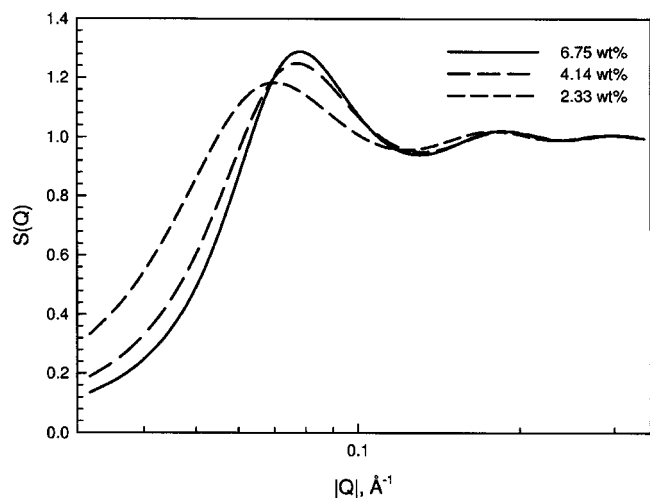


FIG. 5. Calculated structure factor for the monomer-monomer interaction in three  $\beta$ -lg solutions 5 min after the heating had started.

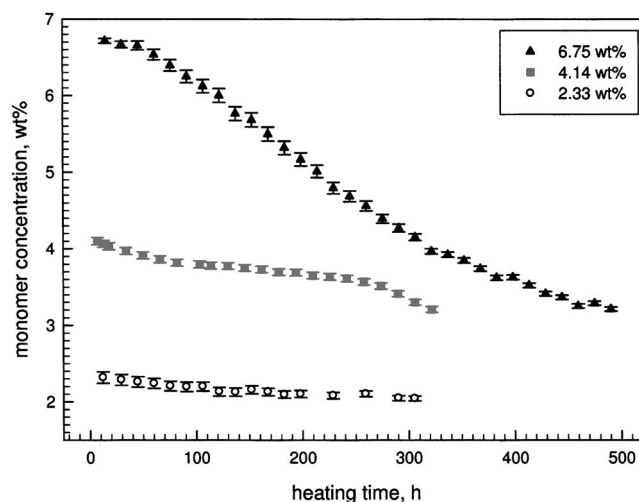


FIG. 6. Data for monomeric protein concentration during the heating of three  $\beta$ -lg solutions, at three different concentrations indicated in the legend, obtained as best-fit parameters from time-resolved SANS data.

to model the kinetics of fibril formation at all times one would need a more complicated model, which would have to be solved numerically.

## CONCLUDING REMARKS

We have studied the kinetics of fibrillar aggregation of  $\beta$ -lg at *pD* 2.0 and low ionic strength by time-resolved SANS. A simple model for the scattering from a solution of monomers and cylindrical fibrils is proposed and a computer program that can fit the experimental data has been written. The model agrees very well with the experimental data, yielding valuable kinetic information about the time dependence of the free monomeric protein concentration and the concentration of protein incorporated in the fibrils. This shows that time-resolved SANS can be used with success in studying protein aggregation and that with enough additional information for the aggregation process one can, in practice, obtain complete information about the aggregation kinetics of the process.

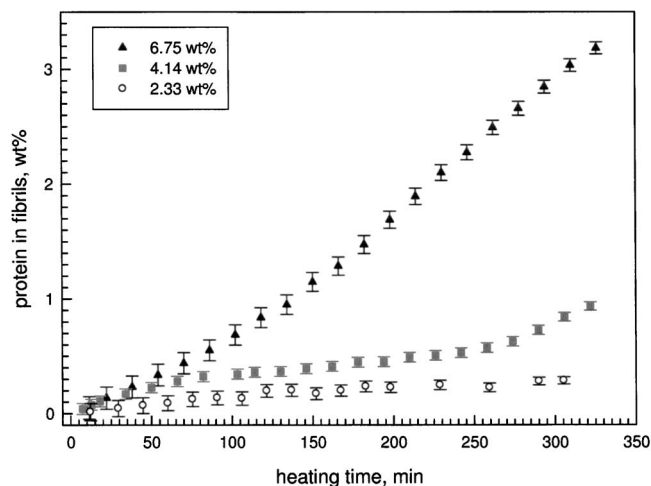


FIG. 7. Data for protein concentration in the fibrils during the heating of three  $\beta$ -lg solutions at three different concentrations indicated in the legend, obtained as best-fit parameters from time-resolved SANS data.

## ACKNOWLEDGMENTS

This work was supported by the Netherlands Research Council for Chemical Sciences (CW) with financial aid from the Netherlands Organization for Scientific Research (NWO), in the context of the SOFTLINK program "Theoretical Biophysics of Proteins in Complex Fluids." The authors thank Joahim Kohlbrecher for assistance with the neutron scattering and Remco Fokkink for his valuable technical expertise.

<sup>1</sup>L. N. Arnaudov, R. de Vries, H. Ippel, and C. P. M. van Mierlo, *Biomacromolecules* **4**, 1614 (2003).

<sup>2</sup>L. N. Arnaudov, Ph.D. thesis, Chap. 3, Wageningen University, 2005.

<sup>3</sup>L. N. Arnaudov, Ph.D. thesis, Chap. 4, Wageningen University, 2005.

<sup>4</sup>M. Verheul, J. S. Pedersen, S. P. F. M. Roefs, and K. G. de Kruif, *Biopolymers* **49**, 11 (1999).

<sup>5</sup>P. Aymard, T. Nicolai, and D. Durand, *Macromolecules* **32**, 2542 (1999).

<sup>6</sup>P. Aymard, D. Durand, and T. Nicolai, *Int. J. Biol. Macromol.* **19**, 213 (1996).

<sup>7</sup>M. A. M. Hoffmann, S. P. F. M. Roefs, M. Verheul, P. J. J. M. van Mil, and K. G. de Kruif, *J. Dairy Res.* **63**, 423 (1996).

<sup>8</sup>M. Verheul, S. P. F. M. Roefs, and K. G. de Kruif, *J. Agric. Food Chem.* **46**, 896 (1998).

<sup>9</sup>N. J. Wagner, R. Krause, A. R. Rennie, B. D'Aguzzo, and J. Goodwin, *J. Chem. Phys.* **95**, 494 (1991).

<sup>10</sup>J. S. Pedersen, *Adv. Colloid Interface Sci.* **70**, 171 (1997).

<sup>11</sup>H. C. Van de Hulst, *Light Scattering by Small Particles* (Dover, New York, 1981).

<sup>12</sup>J. B. Hayter and J. Penfold, *Mol. Phys.* **42**, 109 (1981).

<sup>13</sup>J. P. Hansen and J. B. Hayter, *Mol. Phys.* **46**, 651 (1982).

<sup>14</sup>W. H. Press, B. P. Flannery, S. A. Teukolsky, and W. T. Vetterling, *Numerical Recipes in Pascal*, 2nd ed. (Cambridge University Press, Cambridge, 1992).

<sup>15</sup>W. Cheney and D. Kincaid, *Numerical Mathematics and Computing*, 4th ed. (Brooks-Cole, Belmont, MA, 1999).

<sup>16</sup>S. S. Rogers, P. Venema, L. M. C. Sagis, E. van der Linden, and A. M. Donald, *Macromolecules* **38**, 2948 (2005).